International Immunopharmacology 75 (2019) 105778

Contents lists available at ScienceDirect

International Immunopharmacology

journal homepage: www.elsevier.com/locate/intimp

miR-140-5p regulates T cell differentiation and attenuates experimental autoimmune encephalomyelitis by affecting CD4$^+$T cell metabolism and DNA methylation

Shang Zhu[b,1], Xiaorong Zhang[a,1], Hongbing Guan[a,*], Feng Huang[a], Lihong Wu[a], Dan Hou[a], Zhichao Zheng[a], Miao Yu[a], Liwen Huang[a], Linhu Ge[a]

[a] Key Laboratory of Oral Medicine, Guangzhou Institute of Oral Disease, Stomatology Hospital of Guangzhou Medical University, Guangzhou, Guangdong 510140, China
[b] Guangzhou Medical University, Guangzhou, Guangdong 511436, China

ARTICLE INFO

Keywords:
miRNA
miR-140-5p
Th1
Multiple sclerosis
Experimental autoimmune encephalomyelitis
Methylation
Metabolism

ABSTRACT

We previously demonstrated that decreased expression of miR-140-5p was associated with the progression of multiple sclerosis (MS) and miR-140-5p targeted STAT1 and interfered with the expression of IFN-γ. However, the underlying mechanisms how miR-140-5p regulated the differentiation of encephalomyelitic CD4$^+$T cell remained unclear. In this study, we analyzed the levels of miR-140-5p in a mouse model of experimental autoimmune encephalomyelitis (EAE). We also analyzed the outcomes in response to either over- or under-expression of miR-140-5p. We found that the expression of miR-140-5p was inversely related to the progression of EAE. With the remission of the disease, the expression of miR-140-5p was restored to levels comparable to the control. The expression of miR-140-5p was downregulated in the encephalomyelitic CD4$^+$T cells whereas enhanced expression of miR-140-5p inhibited the development of T helper type 1 (Th1) cell and significantly attenuated EAE. MiR-140-5p also caused hypermethylation of STAT1 and demethylation of GATA3. Furthermore, we found that miR-140-5p enhanced mitochondrial glycolysis in CD4$^+$T cells with simultaneous activation of ATP activity. By blockage of the respiratory electron transport chain with the inhibitors of complex I and III, the effect of miR-140-5p on Th1 differentiation was blocked, which suggested a role for mitochondrial respiratory pathway in miR-140-5p-mediated inhibition of Th1 differentiation. In summary, our results demonstrated that the expression of miR-140-5p was negatively correlated with the progression of EAE and that miR-140-5p regulated Th1 differentiation via DNA methylation and mitochondrial respiratory pathway.

1. Introduction

Multiple sclerosis is an autoimmune neurodegenerative disease of the central nervous system and is characterized by demyelination of nerves and movement of autoreactive lymphocytes [1,2]. Animal model of Experimental Autoimmune Encephalomyelitis (EAE) is widely used to study MS. In EAE, CD4$^+$T cells mediate demyelination and penetration of Th1 and Th17 cells [3,4]. Th1 cells play a crucial role in both MS and EAE and are identified as the main target of both the diseases. The acute phase and the recovery phase of EAE are identified by the presence of cytokines such as IFN-γ which are delivered by Th1 and other autoreactive T cells [3] and which are responsible for the pathology the disease as the primary effectors of the chronic autoimmune inflammation [5]. The development of EAE is dictated by the balance of the effector T cells and the regulatory mechanisms involving different signaling pathways. Expansion of Th1/Th17 cells or reduction of Th2 cells intensifies EAE disease and the presence of diverse cytokine milieu control Th1- or Th2-polarization through signaling via JAK/STAT pathway [6,7]. The Th1 signaling is facilitated by Tbx (T-bet). STAT1 participates in the production of IFN-γ which is regulated by Tbx. Thus, exploring the role of transcription factors critical for Th1 may explain the underlying mechanisms of pathophysiology of EAE. T cell proliferation and differentiation is an energy consuming process and involves biosynthetic pathways. It was found that fatty acid oxidation in mitochondria is a key source of energy to promote the persistence of CD8$^+$T cells and it also promotes the differentiation of T cells directly.

Abbreviation: MS, multiple sclerosis; EAE, experimental autoimmune encephalomyelitis

* Corresponding author.
E-mail address: hongbing2015@qq.com (H. Guan).

[1] S.Z and Z.X equally contribute to the paper.

https://doi.org/10.1016/j.intimp.2019.105778
Received 30 April 2019; Received in revised form 30 June 2019; Accepted 23 July 2019
Available online 05 September 2019

It was also shown that metabolism of $CD4^+$T cells may regulate inflammation in EAE [8,9]. Although some regulators and biomarkers of EAE have been identified, the specific mechanisms of how metabolism influences the progression of EAE remain unclear.

MicroRNAs (miRNAs) are a novel class of short-chain non-coding RNAs which play a vital role in regulating many physiological and pathophysiological processes [10]. They degrade or cause translational inhibition by binding to the 3′UTR (untranslated region) of the mRNAs and are associated with numerous processes such as development, homeostasis, pathophysiological changes and inflammation. MiRNAs have been studied as the targets for diagnosis and as potential treatment strategies for clinical problems [11,12]. Role of microRNAs (miRNAs) has been demonstrated in the pathogenesis of autoimmune diseases, such as miR-146 are dysregulated in human MS. It plays a negative feedback role in TLR4 and cytokine signaling pathways related to TRAF-6 and IRAK-1 [13,14]. On the other hand, higher levels of miR-155 and miR-326 are found in active MS lesions and are associated with the promotion of encephalitogenic Th1 and Th17 cells which are responsible for the development of MS. MiR-155 promotes immune response associated with specific Toll-like receptors and enhances the production of encephalitogenic T cells. MiR-326 targets Est-1 a negative regulator of Th17 differentiation and downregulation of miR-126 alleviated EAE [15,16]. Thus, miRNAs play an important role in the pathogenesis of MS and are emerging as potential biomarkers or targets in the diagnosis and therapeutic strategy in MS, respectively.

MicroRNA miR-140-5p was first discovered in chondrocytes and was linked to cartilage degeneration and ossification [17]. MiR-140-5p has been found to target MMD, Dnmt1, and IFGBP5 and to restrain tumor growth [18–20]. Recent studies have shown the therapeutic role of miR-140-5p in cancer. miR-140-5p was found to target Wnt1 and improved the function of doxorubicin which suppresses the growth of tumor by regulating oncogene expression [21–23]. In a recent study, Guan et al. reported that miR-140-5p expression was negatively correlated with the progression of MS [7]. It was found that the expression of miR-140-5p gradually diminished in the inflammatory $CD4^+$T cells in MS patients but there was no significant change in the number of Th2 cells. Thus, miR-140-5p does not promote differentiation of Th2. Guan et al. also found that miR-140-5p inhibited differentiation of $CD4^+$T cells into Th1 cells during the development of MS and that miR-140-5p suppressed activation of STAT1. However, the precise mechanism how miR-140-5p regulated $CD4^+$T differentiation was not clarified.

In this study, we used mouse EAE model to further investigate the effect of miR-140-5p on the development of Th1 cells. We also explored the effect of miR-140-5p on the metabolic activity and the methylation of STAT1 in $CD4^+$T cells.

2. Materials and methods

2.1. Mice and reagents

C57BL/6 female mice were purchased from Guangdong Medical Laboratory Animal Center. All experimental animals were housed in a specific pathogen-free animal facility at Guangzhou Medical University and used at the age of 6–8 weeks under the protocols approved by the Institute Animal Care and Use Committee of the university. $MOG_{35–55}$ peptide was purchased from GL Biochem (Shanghai, China). Pertussis Toxin was purchased from Tocris. Incomplete Freund's adjuvant was purchased from Sigma. All antibodies and isotype were purchased from ebioscience. Cell stimulation cocktail was purchased from ebioscience.

2.2. Cell isolation

$CD4^+$T cells were purified from the spleen by magnetic separation with EasySep FITC Selection Kit (Stemcell) or by cell sorting with BD Aria III. For the isolation of CNS-infiltrating mononuclear cells (MNCs), mice were perused through heart with 30 ml heparin-PBS. Spinal cord and brain were collected, minced, and centrifuged with 30% Percoll (Sigma) for 15 min and the monocellular layers were harvested.

2.3. EAE induction and adoptive transfer

EAE was induced as described previously [24]. Briefly, 5 mice per group were immunized subcutaneously with 150 μg $MOG_{35–55}$ in CFA containing heat-killed *Mycobacterium tuberculosis* (H37Ra strain, 6 mg/ml). On day 0 and 2 after the immunization, mice were given intraperitoneal injection of 200 ng and 400 ng of pertussis toxin respectively. For adoptive transfer, splenocytes were prepared from virus-infected or uninfected EAE mice on day 8 after the immunization and were treated with $MOG_{35–55}$ peptide (30 μg/ml) for 3 days. $CD4^+$T cells were then purified and 3.0×10^6 cells were transferred to naive mice intravenously. On day 0 and 2 after the transfer, mice were given 200 ng and 400 ng of pertussis toxin, respectively. Mice were examined daily and symptoms of EAE were scored as described previously [24].

2.4. Intracellular staining and flow cytometry

For staining of intracellular IFN-γ, IL-4, and IL-17, splenocytes were either obtained from in vitro culture, or isolated from spleen on day 15 after immunization. Splenocytes were further treated with $MOG_{35–55}$ peptide (30 μg/ml) for 3 days. For intracellular staining, cells were stimulated with Cell Stimulation Cocktail which is a cocktail of phorbol 12-myristate 13-acetate (PMA) and ionomycin for 5 h before staining the surface marker with anti-CD4-PE-Cyanine7. Cells were then fixed, permeabilized, and stained with IFN-γ-FITC, IL-4-PE, and IL-17-APC antibodies as described previously [25]. Cells were analyzed by BD FACS Canto II flow cytometry.

2.5. Lentivirus preparation

Lentiviruses were prepared to overexpress or under express miR-140-5p. The sequences for control (5′-TTCTCCGAACGTGTCACGT-3′), for overexpression of miR-140-5p (5′-CAGTGGTTTTACCCTATGG TAG-3′) and for downregulation of miR-140-5p (5′-CTACCATAGGGTA AAACCACTG-3′) were cloned into lentiviral vector pWPT-GFP or pLVTHM (named as LV-NC, LV-mimic LV-inhibit, respectively). The virus was produced in 293T cells as previously described [26]. 293T cells were cultured in high-glucose DMEM (Gibco) supplemented with 10% FBS (Gibco). Splenocytes were infected with the virus at multiplicity of infection (MOI) of 10 by centrifugation for 60 min at 2000 rpm at room temperature. Lentiviruses (3.0×10^7) were injected intravenously [27].

2.6. Quantitative PCR

Total RNA was isolated with QIAzol lysis reagent (QIAgen). MiRNA was purified with miRNeasy Mini Kit (QIAgen). cDNA was synthesized from 0.3 to 1 μg RNA using Mir-X™ miRNA First-Strand Synthesis kit (Clontech) using manufacturer's protocol. Quantitative PCR (qPCR) was carried out using SYBR® Premix Ex Taq™ II Perfect Real Time kit (TaKaRa) in a 20 μl PCR mixture that included 12.5 μl SYBR® Premix Ex Taq™ II, 2 μl of cDNA template and 0.4μM of each PCR primer (miR-140-5p: 5′-AGTGGTTTTACCCTATGGTAG-3′ and presented in Table 1) according to the manufacturer's protocol. Relative fold changes in miRNA expression were calculated by $2^{-\Delta\Delta ct}$ method using RNU1A as an internal standard control.

2.7. Methylation-specific PCR (MSP)

To examine DNA methylation, methylation-specific PCR was performed as described [28]. Briefly, genomic DNA from $CD4^+$T cells was prepared using TIANamp Genomic Kit (Tiangen, Beijing, China) and further subjected to bisulfite conversion using a DNA Bisulfite

Table 1
Primer sequences of the genes used for qPCR.

Gene	Primer	Primer sequence (5′-3′)
STAT1	STAT1 FP	AACTGCCAACTCAACACC
	STAT1 RP	GTGACAGAGCCCAGGAAT
Tbx	Tbx FP	TGCTGCCTTCTGCCTTTC
	Tbx RP	TTCCCATTCCTGTCCTTCA
GATA3	GATA3 FP	GGTGGGAAGAGTCCAGAGC
	GATA3 RP	GCCAGGCAAGATGAGAAAG
CXCL12	CXCL12 FP	GAAGGGCACAGTTTGGAG
	CXCL12 RP	GTCAGCCTGAGCTACCGA
SMAD3	SMAD3 FP	AAGGGTCCATTCAGGTGTA
	SMAD3 RP	GGGCTTTGAGGCTGTCTA
HDAC4	HDAC4 FP	ACCACAGCAAAGCCATTC
	HDAC4 RP	ACACTCCTCTACGGCACAA

FP = forward primer, RP = reverse primer.

Table 2
Primer sequences of the genes used for MSP.

Gene	Primer	Primer sequence (5′-3′)
STAT1	STAT1MF	TCGGTATTTTCGGTTTTTAGC
	STAT1MR	TCACTACACGCAAAAACTCG
	STAT1UF	TGTTTGGTATTTTTGGTTTTTAGT
	STAT1UR	ACTCACTACACACAAAAACTCAA
Tbx	TbxMF	AGAAACGATGTTGTTGGTTC
	TbxMR	GCCTCGAATAAACATCGTAA
	TbxUF	AGAAGAAATGATGTTGTTGGTTT
	TbxUR	CCCACCTCAAATAAACATCATAA
GATA3	GATA3MF	TGGATTTAGGAAAATAAACGC
	GATA3MR	TACGAAAACTCCGTCAAAAC
	GATA3UF	GTGGATTTAGGAAAATAAATGT
	GATA3UR	CTACAAAAACTCCATCAAAAC
CXCL12	CXCL12MF	GGAAAGGTTCGTAGTTTTGC
	CXCL12MR	GACCCGTAAAACACGAAAA
	CXCL12UF	GGGAAAGGTTTGTAGTTTTGT
	CXCL12UR	CAACCCATAAAACACAAAAA

MF = methylated forward, MR = methylated reverse, UF = unmethylated forward, UR = unmethylated reverse.

Conversion Kit (Tiangen, Beijing, China). MSP was carried out using the Methylation-specific PCR Kit (Tiangen, Beijing, China). All procedures were carried out according to manufacturer's instructions. Methylated and unmethylated DNA primer sequences are presented in Table 2. Primers were generated by using Methyl Primer Express version 1.0 software. The products were analyzed by 1.5% agarose gel and bands were quantified with ImageJ.

2.8. Histopathology

Removing the brain from mice after heparin-PBS perfusion and fixed in 10% paraformaldehyde. The sections of the brain were stained with H&E or Luxol Fast Blue [24] and examined under light microscope.

2.9. Metabolic activity assays

Oxygen consumption rate (OCR; in picomoles per minute) and extracellular acidification rate (ECAR; in milli-pH units per minute) were measured by a Seahorse XF-24 metabolic extracellular flux analyzer (Seahorse Bioscience). $CD4^+$T cells isolated from mice were resuspended in XF assay medium (XF base medium containing 2.5 mM glucose, 2 mM L-glutamine, and 1 mM sodium pyruvate) at pH 7.4 and plated onto 24-well XF microplates (5.0×10^5 cells per well) coated with Corning Cell-Tak adhesive (Corning) following the Seahorse protocol. For XF cell mito- and glycolysis stress test, cells were treated with oligomycin (1 μM), FCCP (1 μM), rotenone (1 μM), antimycin A (1 μM), D-glucose (10 mM), 2-Deoxy-D-glucose (2DG, 50 mM; all from Seahorse Bioscience) following the Seahorse protocol. The results were analyzed with a Seahorse Wave software.

2.10. Statistical analysis

Statistical difference between different groups was analyzed by a two-tailed Student *t*-test or ANOVA test. The nonparametric data (EAE scoring) were analyzed using the Mann-Whitney *U* test. p value < 0.05 was considered statistically significant.

3. Results

3.1. miR-140-5p is downregulated in $CD4^+$T cells in EAE mice

We performed qPCR to examine the levels of miR-140-5p in the splenic $CD4^+$T cells isolated from EAE mice. On the peak of EAE development (day 15 of immunization), we found that the expression of miR-140-5p was significantly decreased in $CD4^+$T cells in comparison to the splenic $CD4^+$T cells isolated from control mice. Moreover, $CD8^+$T cells, CNS-MNCs, and non-T cells also showed a decreased expression of miR-140-5p in EAE mice when compared to the control animals (Fig. 1A). Expression of miR-140-5p in $CD4^+$T cells was found to be inversely proportional to the progression of EAE where the levels of miR-140-5p started to decrease at an early stage of EAE and continued to drop as the disease progressed to a peak stage. Conversely, the levels of miR-140-5p gradually revert back to original levels upon remission of EAE. Interestingly, miR-140-5p expression was higher in $CD4^+$T cells in EAE than the control $CD4^+$T cells in the beginning of remission (Fig. 1B). Taken together, these results suggested that a negative correlation existed between the levels of miR-140-5p and the development of EAE.

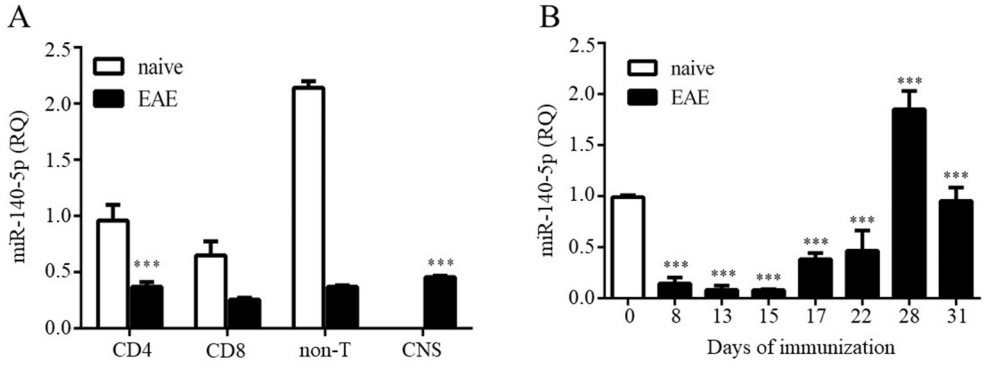

Fig. 1. The expression of miR-140-5p in animal model of EAE. EAE was induced by immunization of $MOG_{35–55}$ peptide in C57BL/6 mice. $CD4^+$T cells and other cell subsets were purified from the spleen of EAE mice following different days of immunization or from the spleen of naive mice using magnetic beads or by sorting with FACS. CNS-MNCs were prepared with Percoll from EAE mice on day 15 of immunization. To analyze the expression of miR-140-5p, qPCR was performed and RNU1A was used to normalize the CT values. (A) Expression of miR-140-5p in $CD4^+$T cells, other cell subsets, and CNS-MNCs on day 15 of immunization in EAE mice or naive mice. (B) Expression of miR-140-5p was compared in $CD4^+$T cells on different days of EAE and $CD4^+$T cells of naive mice (marked as day 0). Data are shown as mean ± SEM (N = 5) from three independent experiments. Values were compared to miR-140-5p expression $CD4^+$T cells of naïve mice ***p < 0.001 (one-way ANOVA test).

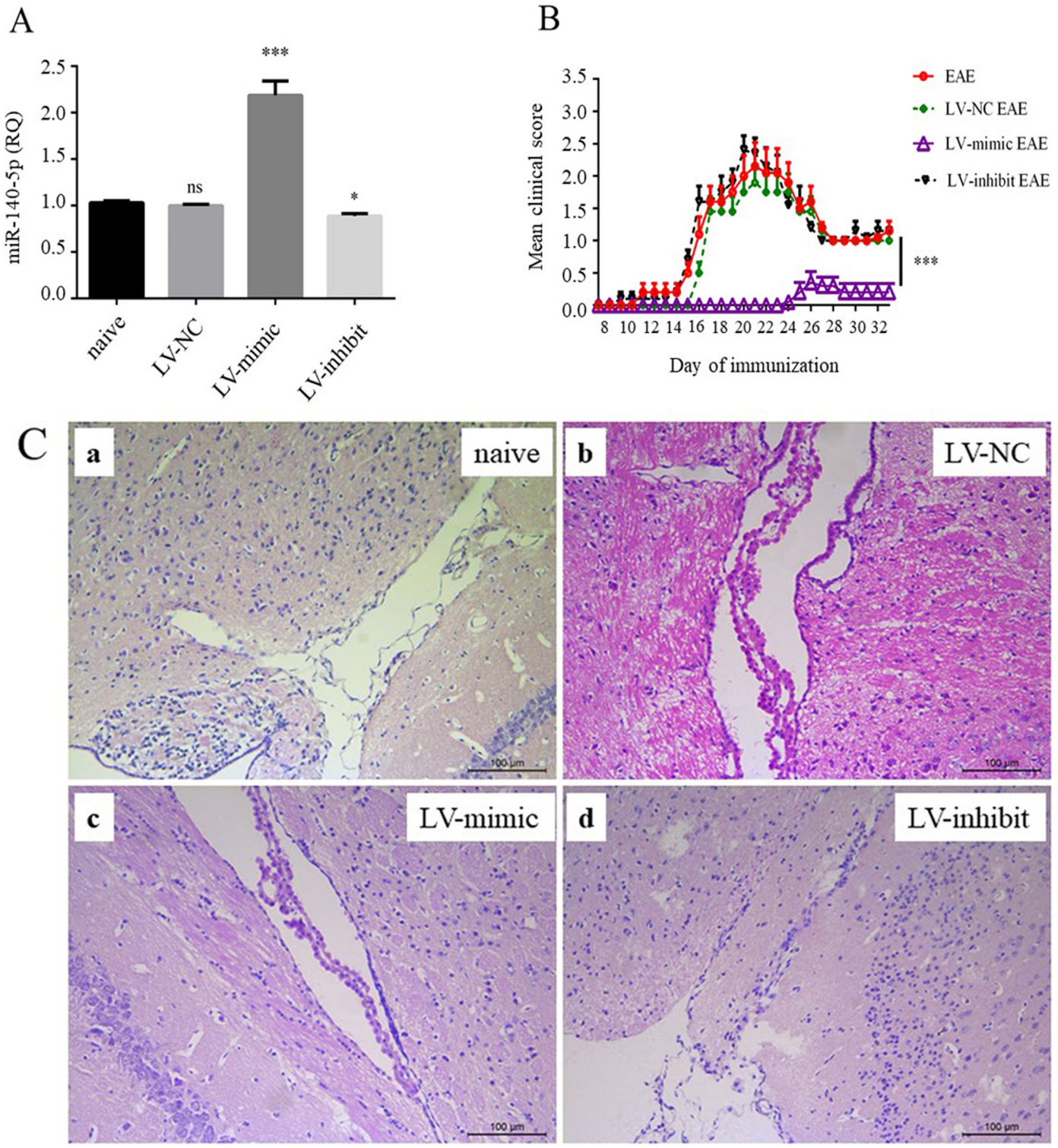

Fig. 2. miR-140-5p suppresses the development of EAE. Naive mice were injected with either LV-mimic, LV-inhibit or LV-NC (3.0×10^7 lentivirus particles per group) intravenously 7 days before immunization. (A) $CD4^+$T cells were isolated from spleens of infected mice after 3 days of injection, and miR-140-5p expression among different groups was analyzed by qPCR. Values were compared to expression in $CD4^+$T cells in naïve mice (one-way ANOVA test). ***$p < 0.001$, *$p < 0.05$, ns: not significant. (B) Mean clinical scores of EAE in different lentivirus-infected mice. Values were compared to those in LV-NC mice (n = 10, Mann-Whitney test to two-way ANOVA in LV-NC and LV-mimic groups). ***$p < 0.001$, (C) H&E staining (a–d) or Luxol fast blue staining (e–h). Brain sections were prepared from naïve mice (a and e) and from EAE mice 20-day post immunization; LV-NC EAE (b and f), LV-mimic EAE (c and g) and LV-inhibit EAE (d and h). (D) Flow cytometry analysis of Th1 differentiation. Values were compared to those in $CD4^+$T cells from LV-NC mice (one-way ANOVA test). **$p < 0.01$, Dot plots of IL-4 and IFN-γ staining and histogram showing the percentage of Th1 population. The gate of dot plots was set on $CD4^+$ population. (E) $CD4^+$T cells from LV-infected mice were transferred into naïve mice of EAE in different groups were analyzed. The mean clinical scores of LV-mimic mice are shown, versus LV-NC (Mann-Whitney test); Th1 cells from splenocytes of the recipient mice were examined by flow cytometry and the values were presented as dot plots and histogram. Values were compared to $CD4^+$T cells from LV-NC mice (one-way ANOVA test). *$p < 0.05$. Data represents mean ± SEM from three independent experiments.

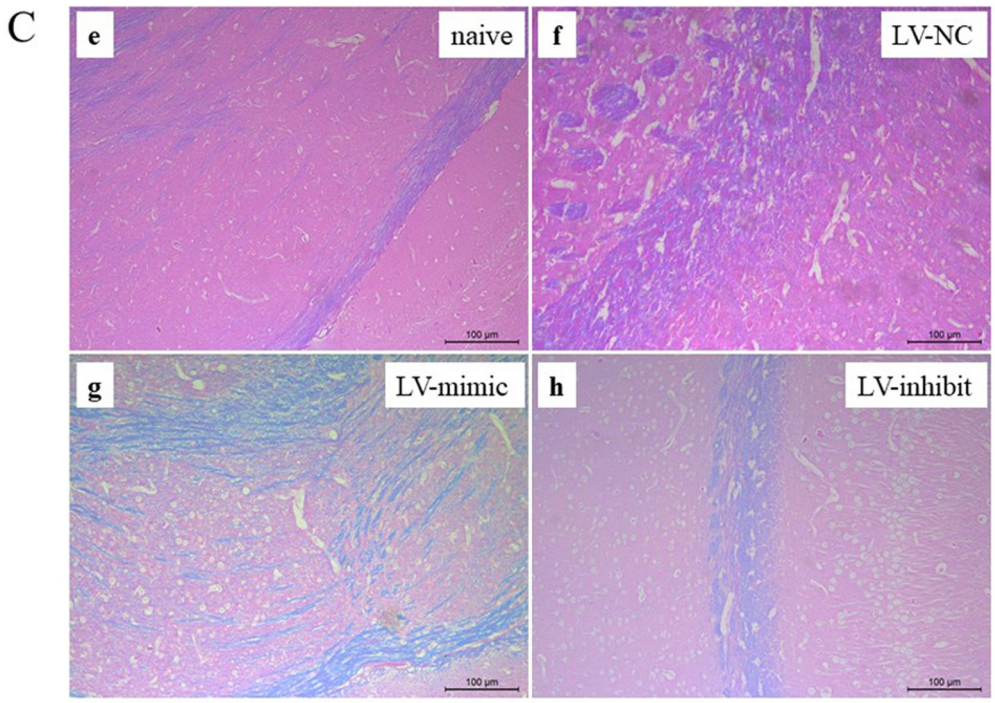

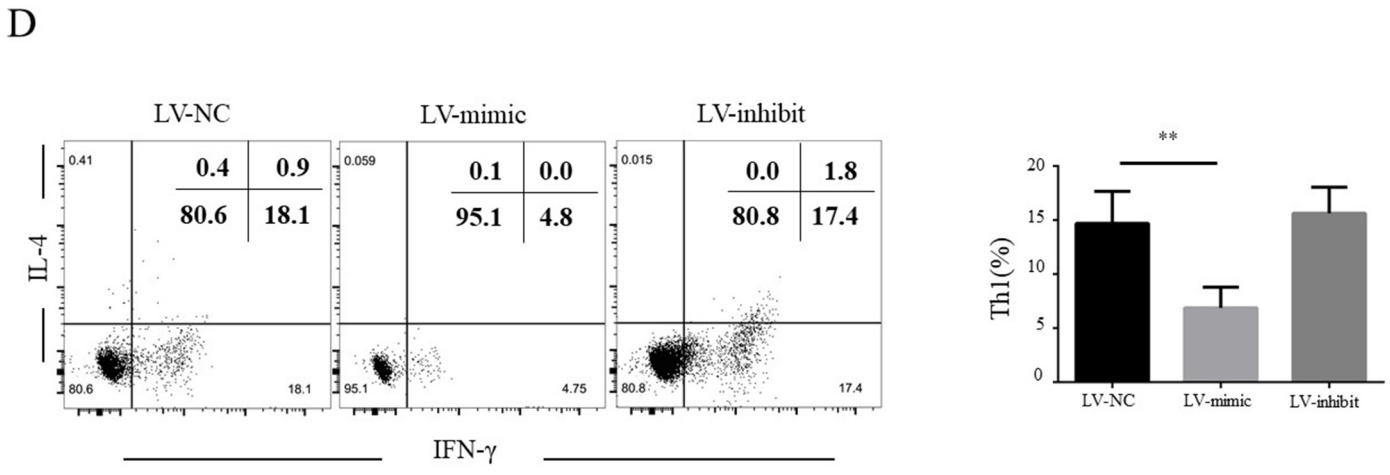

Fig. 2. (*continued*)

3.2. miR-140-5p inhibits Th1 differentiation in EAE mice

To investigate whether the miR-140-5p regulates $CD4^+$T cells differentiation, we constructed lentiviral vectors to either overexpress miR-140-5p (labeled as LV-mimic) or suppress endogenous miR-140-5p (labeled as LV-inhibit) in 293T cells. The negative control vector was labeled as LV-NC (Fig. 2A). We then injected 3.0×10^7 recombinant lentivirus into naive mice intravenously a week before the immunization with MOG peptide 35–55. The data showed that infection of mice with LV-mimic encephalitogenic T cells led to markedly milder signs of EAE (Fig. 2B). Histopathology in EAE mice injected with LV-mimic also showed a decreased inflammation and demyelination in brain when compared to that in EAE LV-NC mice (Fig. 2C). On the day 15 of development of EAE, splenic $CD4^+$T cells continued to express miR-140-5p following LV-mimic infection while the cells infected with LV-inhibit showed a suppression of miR-140-5p. Intracellular cytokine staining showed that the frequency and absolute number of Th1 cells in LV-mimic mice were notably lower than that in $CD4^+$T cell population in control mice (Fig. 2D). To confirm whether miR-140-5p directly affects the encephalitogenesis of effector $CD4^+$T cells, $CD4^+$T cells from the virus-infected EAE mice transferred to the naive mice induced. The mean clinical score showed that LV-mimic mice still developed milder signs of EAE when compared to the LV-NC mice. The results of intracellular cytokine staining also supported that miR-140-5p inhibited Th1 differentiation (Fig. 2E). We further examined the $CD4^+$T cells from CNS-MNCs between the groups of LV-NC and LV-mimic mice and also found that the percentage of Th1 cells in LV-mimic mice were lower than that in LV-NC mice. Meanwhile, the number of Th2 and Th17 cells of LV-mimic mice showed no differences which compared to the population in control mice (Fig. 3).

3.3. miR-140-5p regulates methylation of STAT1 and Tbx in $CD4^+$T cells of EAE mice

We next examined whether miR-140-5p regulates $CD4^+$T cells through epigenetic mechanism. DNA was isolated from $CD4^+$T cells from LV-mimic mice and DNA methylation specific PCR was performed The CpG island methylation of STAT1 and Tbx was analyzed. We found

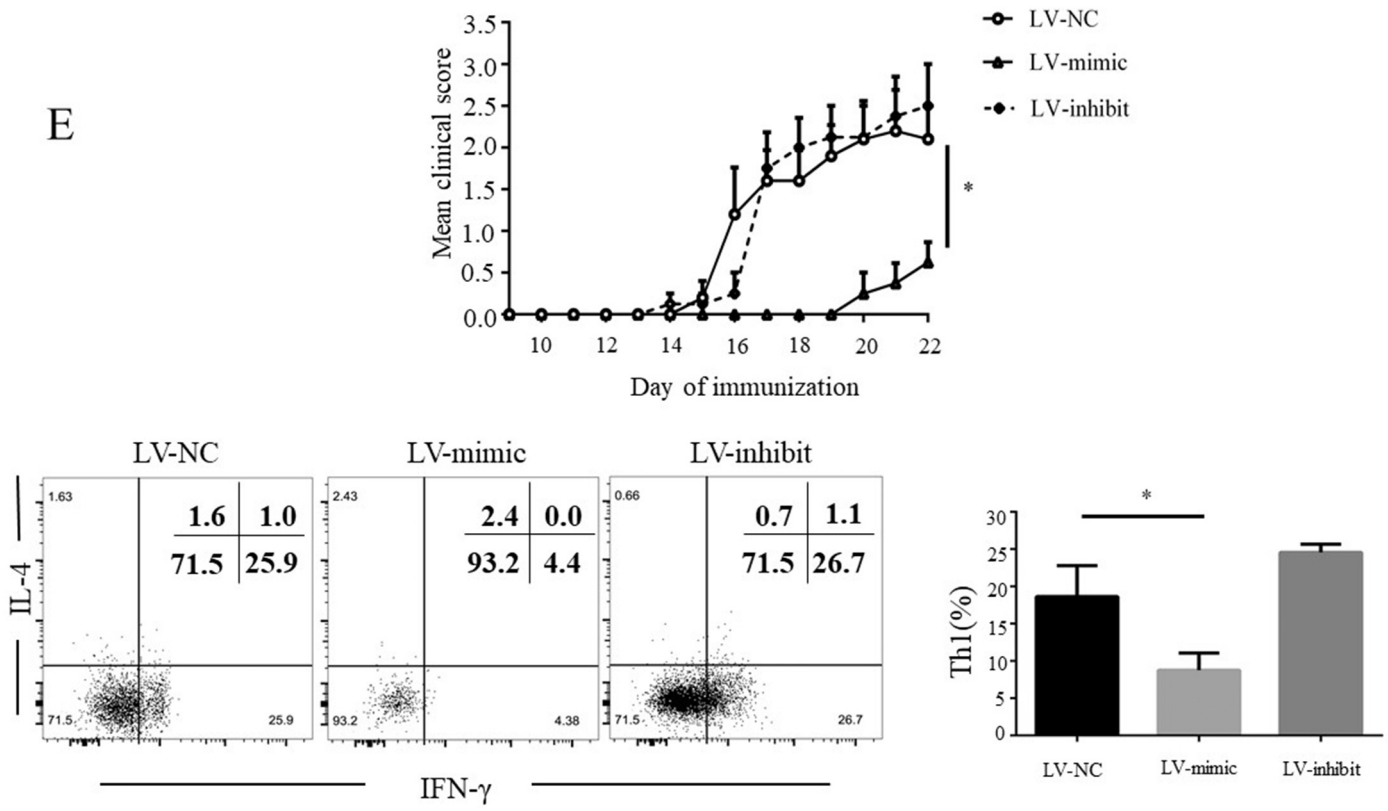

Fig. 2. (*continued*)

that for STAT1, the methylated bands were stronger than the unmethylated band in the samples from EAE mice injected with LV-mimic. Conversely, the intensity of methylated bands was weaker than unmethylated bands in samples from naive, LV-NC, and LV-inhibit mice (Fig. 4A). The results of the Tbx group were similar to those of STAT1 (Fig. 4B). Also, the other target genes of miR-140-5p, GATA3 and CXCL12 showed a significant weaker intensity of methylated bands in comparison to the unmethylated bands in samples from LV-mimic EAE mice suggesting that, GATA3 and CXCL12 were demethylated by miR-140-5p (Fig. 4C–D). These results suggested that miR-140-5p-mediated

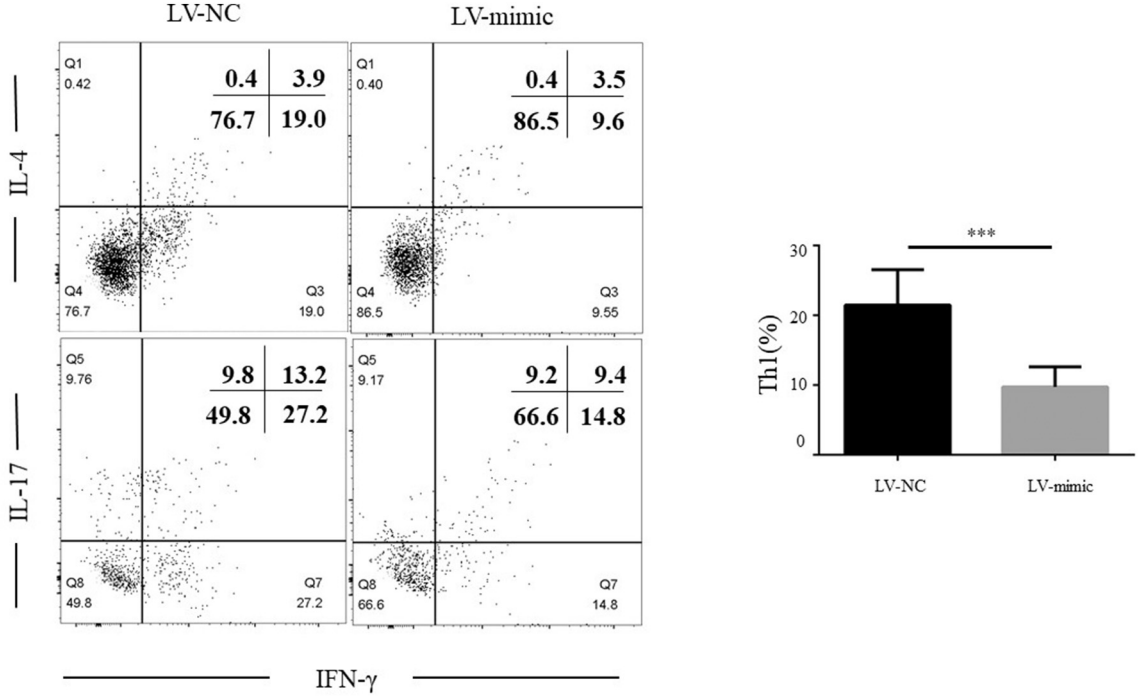

Fig. 3. The differentiation of Th1 cells in CNS regulated by miR-140-5p. CNS-MNCs were isolated from infected EAE mice by Percoll. Th1 cells in CNS-MNCs were detected with flow cytometry. The percentage of Th1 population was shown in dot plots and the gate of dot plots was set on $CD4^+$ population. Values were compared to those in $CD4^+$T cells from the CNS of LV-NC mice (Student's *t*-test), ***$p < 0.001$. Data represents mean ± SEM from three independent experiments.

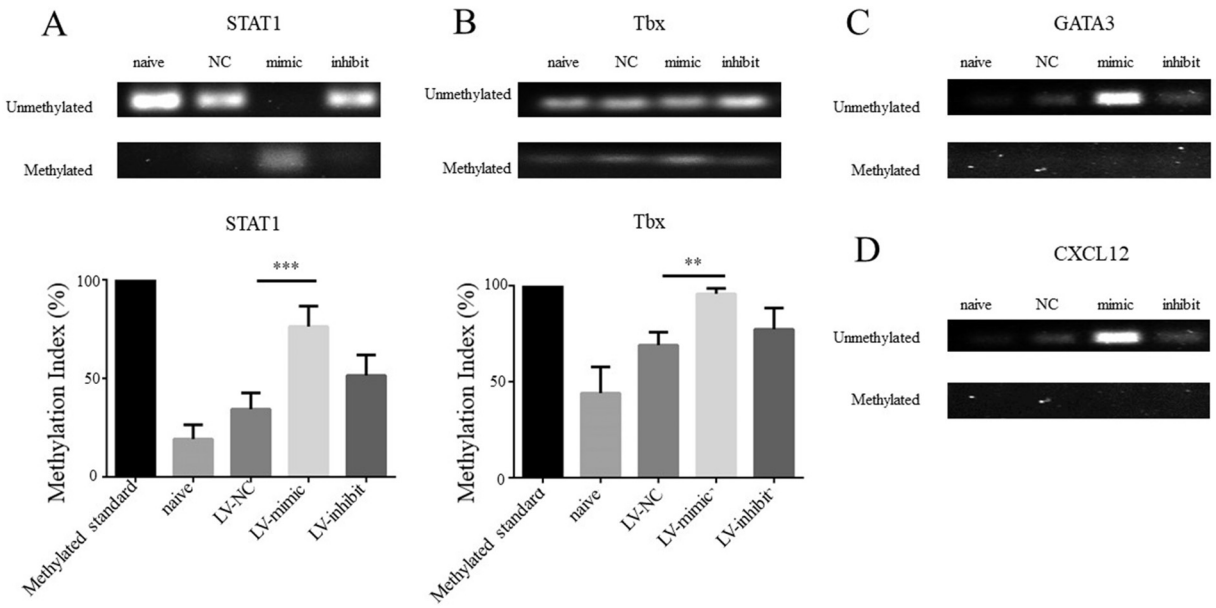

Fig. 4. The CpG island methylation of target genes. Genomic DNA was isolated from CD4$^+$T cells from different groups of mice and was converted by bisulfite-conversion. (A–D) Methylation status in EAE mice infected with LV-NC, LV-mimic, or LV-inhibit group on day 15 post immunization. Universally methylated mouse genomic DNA was used as control. The bands of methylated PCR product (STAT1, Tbx, CXCL12 and GATA3) and methylation index for STAT1 and Tbx are presented. Data (mean ± SEM) from three replicate experiments are shown; **$p < 0.05$, ***$p < 0.001$, one-way ANOVA test.

suppression of Th1 cells was associated with the methylation of STAT1 and Tbx CpG islands.

3.4. miR-140-5p down-regulates the expression of STAT1 in CD4$^+$T cells of EAE mice

To investigate whether the methylation of the genes was related to their expression, we further examined the expression of these genes with the manipulation of miR-140-5p level using lentivirus vectors. The results showed that the expression of STAT1 and Tbx were down-regulated in LV-mimic mice, which were the two genes we found that the methylation of their CpG islands was regulated by miR-140-5p. Moreover, the results showed the downregulation of GATA3, CXCL12 and SMAD3 in LV-mimic mice (Fig. 5). Together, it indicated miR-140-5p was involved in the pathway which decreased the expression of STAT1, Tbx, GATA3, CXCL12 and SMAD3.

3.5. miR-140-5p promotes metabolic activity in CD4$^+$T cells in EAE mice and affects mitochondrial oxidative respiration

We measured the oxygen consumption rate (OCR) and extracellular acidification rate (ECAR) to evaluate the effect of miR-140-5p on mitochondrial oxidative respiration and glycolytic flux in CD4$^+$T cells isolated from different groups of mice. In mito-stress test, the OCR levels in cells from LV-mimic group were upregulated and were higher than other groups in the presence of oligomycin, FCCP, and rotenone and antimycin A (Fig. 6A). We also found that LV-mimic group had the highest level of the proton leak, ATP production, and respiratory capacity when compared to the other two groups, as indicated by the OCR values (Fig. 6B and C). Rotenone and antimycin A inhibit complex I and III of electron transport chains, respectively [29]. Following treatment of cells with rotenone and antimycin A, we found that mito-stress activity was completely blocked and OCR dropped to lowest level in the LV-mimic group when compared to the other groups. These data demonstrated that infecting the mice with LV-mimic improved the mitochondrial oxidative respiration in CD4$^+$T cells.

In glycolysis stress test, the ECAR level was higher in in LV-mimic group in comparison to the other groups following different treatments. Oligomycin binds ATP synthase and inhibits mitochondrial ATP production. Following the treatment with glucose and oligomycin, ECAR was highest in LV-mimic group when compared to other groups. The histogram depicting the ECAR value in all groups indicated an increased metabolic profile of LV-mimic CD4$^+$T cells. Next, we treated the cells with 2-DG, a competitive compound which inhibits hexokinase. We found that, glycolysis was blocked and ECAR dropped to lowest levels in LV-mimic group when compared to the other groups. Meanwhile, CD4$^+$T cells from LV-mimic group still showed a higher ECAR value than the naive mice or EAE mice which were injected with LV-NC and LV-inhibit virus after the treatment of 2-DG. These results indicated that LV-mimic infection increased glycolysis in CD4$^+$T cells by improving the utilization of glucose (Fig. 6D, E).

To further confirm whether miR-140-5p regulated Th1 differentiation by affecting the metabolic status of CD4$^+$T cells, we used 2-DG or rotenone and antimycin A to alter the metabolic status of the splenocytes prepared from EAE mice infected with LV-NC and LV-mimic. Cells were stimulated with MOG, 2-DG or rotenone and antimycin A for 3 days. Flow cytometry analysis showed a lower percentage of Th1 cells in LV-mimic group in comparison to the LV-NC group. However, when rotenone and antimycin A were added to the cells, the percentage of Th1 cells in LV-mimic group increased and was found higher than the other groups. The population of dot plots indicated that rotenone and antimycin A enhanced Th1 differentiation and overcame the inhibitory effect of miR-140-5p on Th1 differentiation. However, we did not see a similar trend with 2-DG (Fig. 7). These results demonstrated that miR-140-5p regulates Th1 differentiation by regulating mitochondrial oxidative respiration and possibly shared common targets with rotenone and antimycin A in the regulation of metabolism and inhibition of Th1 differentiation.

4. Discussion

In this study, we demonstrated that miR-140-5p was downregulated in CD4$^+$T cells in EAE mice which was correlated to the pathogenesis of experimental autoimmune encephalomyelitis. In a recent study, it was shown that miR-140-5p inhibits Th1 differentiation in MS. These findings reveal microRNAs as novel targets for developing effective

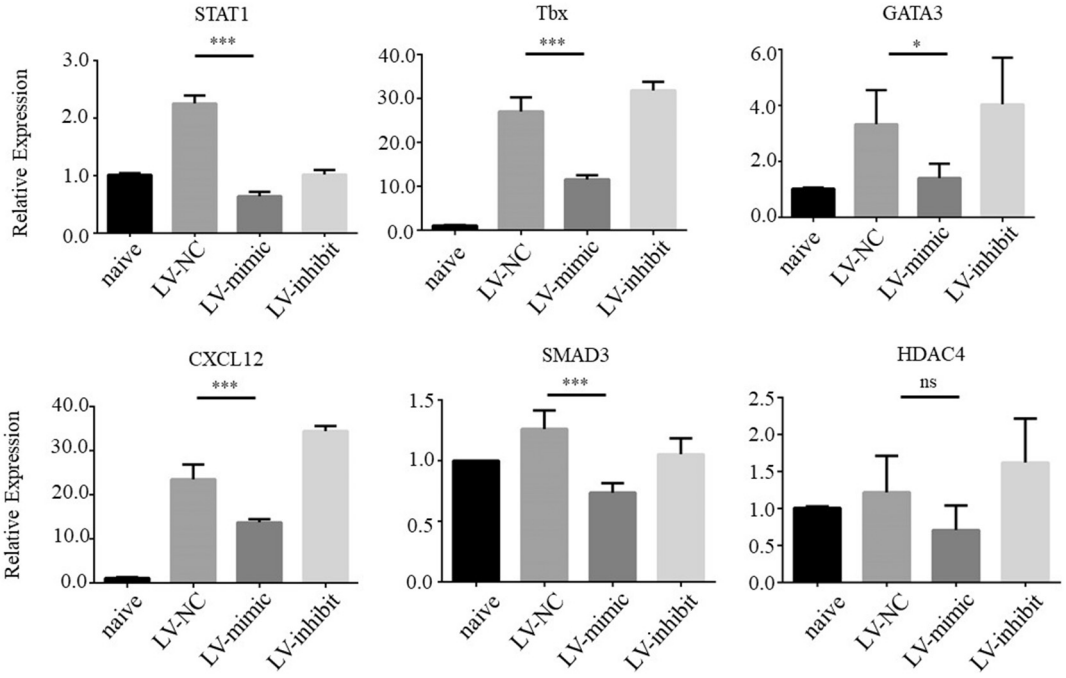

Fig. 5. The expression of target genes. The gene expression in CD4$^+$T cells from the different groups of mice was detected by qPCR. Values were compared to expression in CD4$^+$T cells in naïve mice, ***p < 0.001, *p < 0.05, ns: not significant (one-way ANOVA test).

strategies for treating MS [7]. It has been demonstrated that many miRNAs such as miR-155, miR-326, miR-20b and let-7e affect the pathogenesis of EAE by regulating Th1, Th2 or Th17 cells. In this study, we show that miR-140-5p inhibits differentiation of CD4$^+$T cells by causing methylation of Tbx and Stat1 CpG islands. Also, miR-140-5p improved the energy costs of CD4$^+$T cells and regulate the oxidative respiration.

MiR-140 was first demonstrated to be expressed in tissue-specific manner in zebrafish embryos and in a cartilage-specific manner in mouse embryos [30,31]. Interestingly, miR-140-5p is reported as a putative suppressor in many diseases. Recent studies showed that miR-140-5p plays an important role in regulating the development of certain kinds of cancer by targeting ADAMTS5, IGFBP5, Notch1, IGF2BP1, YES1 [32–35]. MiR-140-5p suppressed the development of T-cell acute lymphoblastic leukemia by regulating TAL1 expression [36]. In the cardiovascular system, the myocardial oxidative stress mediated by miR-140-5p plays an important role in the regulation of dioscin and doxorubicin-mediate cardiotoxicity [37,38]. In the skeletal system, miR-140-5p participates in the development of osteoblasts through MAPK pathway [39]. It was also shown that miR-140 was expressed in differentiated chondrocytes and that overexpression of miR-140-5p regulated the function of articular chondrocytes [40]. Likewise, our results confirmed that miR-140-5p inhibited generation of Th1 and ameliorated the pathogenesis of EAE. We found that miR-140-5p expression was dramatically decreased in encephalitogenic cells and a negative correlation was found between miR-140-5p expression and the development of EAE. Moreover, overexpression of miR-140-5p attenuated the disease by inhibiting differentiation of encephalitogenic CD4$^+$T cells to Th1 cell type.

Signal transducer and activator of transcription 1 (STAT1), a member of the STAT protein family, plays a critical role in Th1 cell differentiation. Tbx regulates STAT1 signaling processes and also plays an important role in Th1 development. It has been demonstrated that overexpression of miR-140-5p inhibits Tbx expression, a downstream target of STAT1, which results in suppression of Th1 differentiation of [41]. DNA methylation is an epigenetic modification which occurs mostly in CpG islands and involves genes silencing. CpG islands are short DNA sequences with an elevated CpG density and GC content. They are typically nonmethylated but become methylated upon silencing of the associated promoters. The mechanisms of DNA methylation-mediated gene silencing is associated with methyl-CpG-binding proteins or DNA binding protein, however, the mechanisms of DNA methylation directing specific sequences of genome remain unclear [42,43]. Recently, it was reported that under the conditions of inflammation, a locus-specific reversible DNA methylation of *Il-10* gene locus mediated its expression in Th1 cells [44].

In the present study, we investigated whether the miR-140-5p was downregulated in EAE. Importantly, we found that overexpression of miR-140-5p inhibited encephalitogenic Th1 cells. Furthermore, we showed that overexpression of miR-140-5p caused methylation of STAT1 and Tbx and demethylation of GATA3 and CXCL12 suggesting that it may act as an epigenetic regulator of these genes. Our results were consistent with previous work which demonstrated that miR-140-5p inhibited STAT1 activation and promoted the increase in the number of GATA3$^+$ CD4$^+$T cells [7]. Another study has demonstrated that has CXCL12 is a direct target of miR-140-5p [45].CXCL12 (CXC chemokine ligand 12, also known as stromal cell-derived factor-1) is important for the development and pathophysiology of diseases of circulatory, immune, and nervous systems.

In our study, we found that miR-140-5p down-regulated STAT1, CXCL12 and SMAD3 directly. It indicated that miR-140-5p suppressed the expression STAT1 and its downstream target, Tbx. The methylation of STAT1 and Tbx CpG islands must played an important role in the regulation of miR-140-5p. Thus, miR-140-5p may play a regulatory role in Th1 differentiation by an epigenetic mechanism. However, overexpression of miR-140-5p caused CXCL12, HDAC4 and its downstream target, GATA3 downregulated which showed no methylation in our study. Together, we indicated that regulating the methylation of DNA CpG islands was one of the pathways induced by miR-140-5p inhibiting the expression of STAT1 and Tbx. In previous study, it is demonstrated that IFN-γ, STAT1 and Tbx signaling pathways played an important role in Th1 cell differentiation, and found the correlation of expression of miR-140-5p with GATA3$^+$ Tbet$^+$ CD4$^+$T cells [7]. Thus, based on these studies, we hypothesize that miR-140-5p regulated the methylation or demethylation of Tbx or GATA3 by regulating the production of IFN-γ and decreasing the expression of STAT1 or SMAD3.

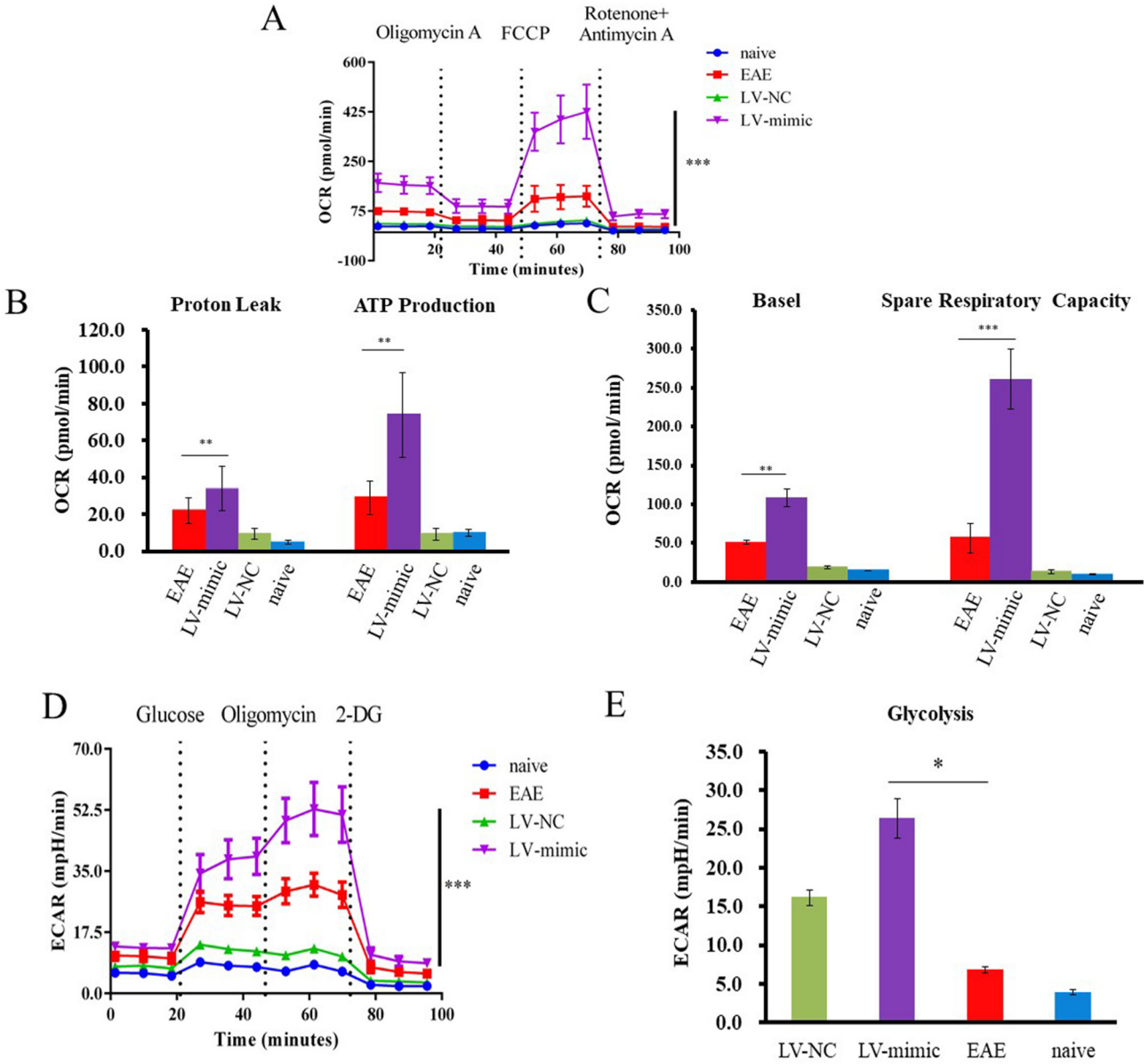

Fig. 6. Correlation between miR-140-5p expression and metabolic activity in $CD4^+$T cells in EAE mice. (A–E) $CD4^+$T cells were isolated from naive mice and from 3 groups of EAE mice on day 15 post-immunization. Oxygen consumption rate (OCR) and extracellular acidification rate (ECAR) were measured by an extracellular flux analyzer. The data in (A) was used to calculate: Basal OCR and spare respiratory capacity (B); Proton leak and ATP production (C). The data in (D) was used to calculate glycolysis ECAR (E). Values were compared to $CD4^+$T cells in EAE mice Data represents mean ± SEM from three independent experiments, *p < 0.05, **p < 0.01, and ***p < 0.001 (one-way ANOVA test).

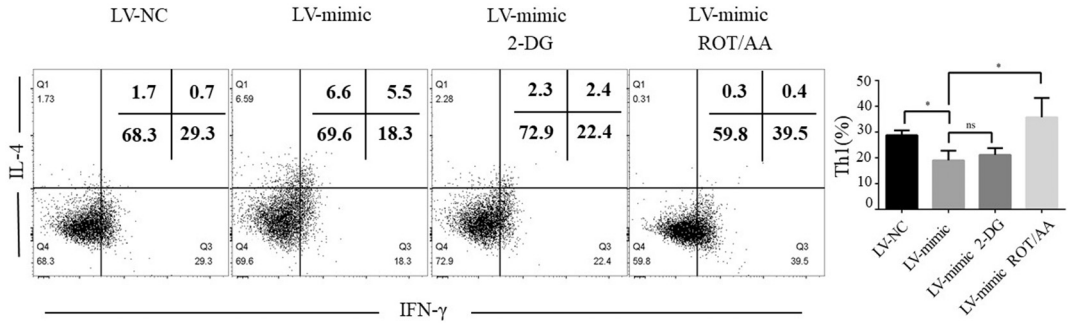

Fig. 7. Rotenone and antimycin A inhibit the function of miR-140-5p during the Th1 differentiation. Splenocytes were prepared on day 15 post-immunization, infected with either LV-NC or LV-mimic and stimulated with $MOG_{35–55}$, 2DG, rotenone and antimycin A. After 3 days of stimulation, Th1 cells were detected by flow cytometry. The dot plots and percentage of Th1 cells are shown. Data represents mean ± SEM from three independent experiments. *p < 0.05; ns: not significant, one-way ANOVA test.

Further, the metabolic activity assays showed that miR-140-5p may induce mitochondrial biogenesis in $CD4^+$T cells. We found that miR-140-5p improved the rate of glycolysis and mitochondrial respiratory capacity. Comparing $CD4^+$T cell differentiation in response to LV-mimic in the presence of various drugs, we found that 2-DG did not show a significant effect. However, rotenone and antimycin A suppressed the function of miR-140-5p and the number of Th1 cells in this group was similar to that in EAE mice infected with LV-NC. These findings suggest that miR-140-5p regulates Th1 differentiation possibly by targeting complex I and III of the electron transport chain. A study showed that miR-140-5p was located in the mitochondria [46]. Generally, miRNAs are synthesized in the nucleus, however, the mature miRNAs can be transported to various compartments including the mitochondria [47]. Glutamine and α-ketoglutarate (αKG) play a crucial role in the differentiation of naïve $CD4^+$T cells by generating Tbx. Decreasing the intracellular concentration of glutamine and its metaboliteαKG was found to inhibit the differentiation of naïve $CD4^+$T cells into Th1 cells [9]. Moreover, TET2, which belongs to the family of ten-eleven-translocation (TET) proteins and which is a αKG-dependent enzyme, increased the number of Th1 cells by mediating DNA methylation and IL-10 production [48]. Our findings suggested that miR-140-5p was involved in the tricarboxylic acid (TCA) cycle which in turn regulated the methylation of transcription factors that mediated $CD4^+$T cell differentiation. These findings may explain regulatory effects of miR-140-5p on Th1 cells but not Th2 cells.

As the conditions in our experimental settings were not hypoxic, we could not determine whether improvement in glycolysis in $CD4^+$T cells regulated their differentiation. Further studies are needed to address this possibility. It has been reported that miR-140-5p and let-7e regulate differentiation of encephalitis T cells. Thus, future studies should focus on the combined function of miR-140-5p and let-7e in regulating the transcription factors and cytokines that participate in the pathogenesis of MS and EAE. Also, the correlation between miRNAs and DNA methylation involving metabolic regulation in T cell differentiation needs further investigation and may provide a potential avenue for immunotherapies.

Financial support

This project was supported by the following sources: Guangzhou Science, Technology and Innovation Commission (grant number: 201707010026), Guangdong Science and Technology Department (grant number: 2017A020215141), Guangzhou Liwan Science Technology Industry Commerce and Information Bureau (grant number: 2016080053), Guangzhou Medical University High-level University Construction Project (Immunology) (grant number: B15001001), Bureau of Health of Guangzhou Municipality (grant number: 20181A011101).

References

[1] L.H. Kasper, J. Shoemaker, Multiple sclerosis immunology, Neurology 24 (12) (2010) 1225–1228.
[2] J. Goverman, Autoimmune T cell responses in the central nervous system, Nat Rev Immunol 9 (6) (2009) 393–407.
[3] A. Jager, V. Dardalhon, R.A. Sobel, E. Bettelli, V.K. Kuchroo, Th1, Th17, and Th9 effector cells induce experimental autoimmune encephalomyelitis with different pathological phenotypes, J. Immunol. 183 (11) (2009) 7169–7177.
[4] M. Elbehi, A. Rostami, B. Ciric, Current views on the roles of Th1 and Th17 cells in experimental autoimmune encephalomyelitis, J. NeuroImmune Pharmacol. 5 (2) (2010) 189–197.
[5] E. Bettelli, T. Korn, M. Oukka, V.K. Kuchroo, Induction and effector functions of T(H)17 cells, Nature 453 (7198) (2008) 1051–1057.
[6] R. Isabella, M. Mathias, D. Thomas, The regulation of inflammation by interferons and their STATs, JAK-STAT 2 (1) (2013) e23820.
[7] H. Guan, U.P. Singh, R. Rao, D. Mrelashvili, S. Sen, H. Hao, et al., Inverse correlation of expression of microRNA-140-5p with progression of multiple sclerosis and differentiation of encephalitogenic T helper type 1 cells, Immunology 147 (4) (2016) 488–498.
[8] G.W. Vanderwindt, B. Everts, C.H. Chang, J. Curtis, T. Freitas, E. Amiel, et al., Mitochondrial respiratory capacity is a critical regulator of CD8 + T cell memory development, Immunity 36 (1) (2012) 68–78.
[9] D. Klysz, X. Tai, P.A. Robert, M. Craveiro, G. Cretenet, L. Oburoglu, et al., Glutamine-dependent α-ketoglutarate production regulates the balance between T helper 1 cell and regulatory T cell generation, Sci. Signal. 8 (396) (2015) ra97.
[10] D.P. Bartel, MicroRNA target recognition and regulatory functions, Cell 136 (2) (2009) 215–233.
[11] M.S. Ebert, P.A. Sharp, Roles for microRNAs in conferring robustness to biological processes, Cell 149 (3) (2012) 515–524.
[12] R. Dai, S.A. Ahmed, MicroRNA, a new paradigm for understanding immunoregulation, inflammation, and autoimmune diseases, Transl. Res. 157 (4) (2011) 163–179.
[13] J.Q. Chen, G. Papp, P. Szodoray, M. Zeher, The role of microRNAs in the pathogenesis of autoimmune diseases, Autoimmun. Rev. 15 (12) (2016) 1171–1180.
[14] K.D. Taganov, M.P. Boldin, K.J. Chang, D. Baltimore, NF-κB-dependent induction of microRNA MiR-146, an inhibitor targeted to signaling proteins of innate immune responses, Proc. Natl. Acad. Sci. U. S. A. 103 (33) (2006) 12481.
[15] R.M. O'Connell, D. Kahn, W.S. Gibson, J.L. Round, R.L. Scholz, A.A. Chaudhuri, et al., MicroRNA-155 promotes autoimmune inflammation by enhancing inflammatory T cell development, Immunity 33 (4) (2010) 607–619.
[16] C. Du, C. Liu, J. Kang, G. Zhao, Z. Ye, S. Huang, et al., MicroRNA miR-326 regulates TH-17 differentiation and is associated with the pathogenesis of multiple sclerosis, Nat. Immunol. 10 (12) (2009) 1252–1259.
[17] S. Hwang, S.K. Park, H.Y. Lee, S.W. Kim, J.S. Lee, E.K. Choi, et al., miR-140-5p suppresses BMP2-mediated osteogenesis in undifferentiated human mesenchymal stem cells, FEBS Lett. 588 (17) (2014) 2957.
[18] A. Takata, M. Otsuka, T. Yoshikawa, T. Kishikawa, Y. Hikiba, S. Obi, et al., MicroRNA-140 acts as a liver tumor suppressor by controlling NF-κB activity by directly targeting DNA methyltransferase 1 (Dnmt1) expression, Hepatology 57 (1) (2013) 162–170.
[19] W. Li, F. He, Monocyte to macrophage differentiation-associated (MMD) targeted by miR-140-5p regulates tumor growth in non-small cell lung cancer, Biochemical & Biophysical Research Communications 450 (1) (2014) 844–850.
[20] G. Güllü, I. Peker, A. Haholu, F. Eren, Z. Küçükodaci, B. Güleç, et al., Clinical significance of miR-140-5p and miR-193b expression in patients with breast cancer and relationship to IGFBP5, Genetics & Molecular Biology 38 (1) (2015) 21–29.
[21] D. Wu, J. Zhang, L. Ying, B. Song, L. Li, W. Lu, et al., miR-140-5p inhibits the proliferation and enhances the efficacy of doxorubicin to breast cancer stem cells by targeting Wnt1, Cancer Gene Ther. 26 (3) (2019) 74–82.
[22] H. Zhai, A. Fesler, Y. Ba, S. Wu, J. Ju, Inhibition of colorectal cancer stem cell survival and invasive potential by hsa-miR-140-5p mediated suppression of Smad2 and autophagy, Oncotarget 6 (23) (2015) 19735–19746.
[23] V. Flamini, W.G. Jiang, Y. Cui, Therapeutic role of MiR-140-5p for the treatment of non-small cell lung cancer, Anticancer Res. 37 (8) (2017) 4319.
[24] H. Guan, P.S. Nagarkatti, M. Nagarkatti, CD44 reciprocally regulates the differentiation of encephalitogenic Th1/Th17 and Th2/regulatory T cells through epigenetic modulation involving DNA methylation of cytokine gene promoters, thereby controlling the development of experimental autoimmune encephalomyelitis, J. Immunol. 186 (12) (2011) 6955–6964.
[25] Z. Yin, D.T. Zhang, G. Bahtiyar, S. Jung, L. Liu, X. Fu, et al., Dominance of IL-12 over IL-4 in gamma delta T cell differentiation leads to default production of IFN-gamma: failure to down-regulate IL-12 receptor beta 2-chain expression, J. Immunol. 164 (6) (2000) 3056–3064.
[26] D. Fan, S. Qiu, C.D. Overton, P.G. Yancey, L.L. Swift, W.G. Jerome, et al., Impaired secretion of apolipoprotein E2 from macrophages, J. Biol. Chem. 282 (18) (2007) 13746–13753.
[27] H. Guan, D. Fan, D. Mrelashvili, H. Hao, N.P. Singh, U.P. Singh, et al., MicroRNA let-7e is associated with the pathogenesis of experimental autoimmune encephalomyelitis, Eur. J. Immunol. 43 (1) (2013) 104–114.
[28] J.M. Sido, X. Yang, P.S. Nagarkatti, M. Nagarkatti, Δ9 tetrahydrocannabinol-mediated epigenetic modifications elicit myeloid-derived suppressor cell activation via STAT3/S100A8, J. Leukoc. Biol. 97 (4) (2015) 677–688.
[29] D.A. Christie, M. Panagiotis, B. Julianna, S.D. Dunn, S.P. Julie, R.G. Jones, et al., Stomatin-like protein 2 deficiency in T cells is associated with altered mitochondrial respiration and defective CD4+ T cell responses, J. Immunol. 189 (9) (2012) 4349.
[30] E. Wienholds, W.P. Kloosterman, E. Miska, E. Alvarezsaavedra, E. Berezikov, B.E. De, et al., MicroRNA expression in zebrafish embryonic development, Science 309 (5732) (2005) 310–311.
[31] L. Tuddenham, G. Wheeler, S. Ntounia-Fousara, J. Waters, M.K. Hajihosseini, I. Clark, et al., The cartilage specific microRNA-140 targets histone deacetylase 4 in mouse cells, FEBS Lett. 580 (17) (2006) 4214–4217.
[32] L. Yu, Y. Lu, X. Han, W. Zhao, J. Li, J. Mao, et al., microRNA-140-5p inhibits colorectal cancer invasion and metastasis by targeting ADAMTS5 and IGFBP5, Stem Cell Res Ther 7 (1) (2016) 180.
[33] P. Jing, N. Sa, X. Liu, X. Liu, W. Xu, MicroR-140-5p suppresses tumor cell migration and invasion by targeting ADAM10-mediated Notch1 signaling pathway in hypopharyngeal squamous cell carcinoma, Exp. Mol. Pathol. 100 (1) (2016) 132–138.
[34] Z. Fang, S. Yin, R. Sun, S. Zhang, M. Fu, Y. Wu, et al., miR-140-5p suppresses the proliferation, migration and invasion of gastric cancer by regulating YES1, Mol. Cancer 16 (1) (2017) 139.
[35] Y. Su, J. Xiong, J. Hu, X. Wei, X. Zhang, L. Rao, MicroRNA-140-5p targets insulin like growth factor 2 mRNA binding protein 1 (IGF2BP1) to suppress cervical cancer growth and metastasis, Oncotarget 7 (42) (2016) 68397–68411.
[36] N.C. Correia, A. Melão, V. Póvoa, L. Sarmento, M.G.D. Cedrón, M. Malumbres, et al., microRNAs regulate TAL1 expression in T-cell acute lymphoblastic leukemia, Oncotarget 7 (7) (2016) 8268–8281.

[37] L. Zhao, Y. Qi, L. Xu, X. Tao, X. Han, L. Yin, et al., MicroRNA-140-5p aggravates doxorubicin-induced cardiotoxicity by promoting myocardial oxidative stress via targeting Nrf2 and Sirt2, Redox Biol. 15 (C) (2018) 284.
[38] L. Zhao, X. Tao, Y. Qi, L. Xu, L. Yin, J. Peng, Protective effect of dioscin against doxorubicin-induced cardiotoxicity via adjusting microRNA-140-5p-mediated myocardial oxidative stress, Redox Biol. 16 (2018) 189.
[39] W. Luo, L. Liu, L. Yang, Y. Dong, T. Liu, X. Wei, et al., The vitamin D receptor regulates miR-140-5p and targets the MAPK pathway in bone development, Metabolism Clinical & Experimental 85 (2018) 139.
[40] S.C. Tao, T. Yuan, Y.L. Zhang, W.J. Yin, S.C. Guo, C.Q. Zhang, Exosomes derived from miR-140-5p-overexpressing human synovial mesenchymal stem cells enhance cartilage tissue regeneration and prevent osteoarthritis of the knee in a rat model, Theranostics 7 (1) (2017) 180–195.
[41] M. Afkarian, J.R. Sedy, J. Yang, N.G. Jacobson, N. Cereb, S.Y. Yang, et al., T-bet is a STAT1-induced regulator of IL-12R expression in naive CD4+ T cells, Nat. Immunol. 3 (6) (2002) 549–557.
[42] A. Portela, M. Esteller, Epigenetic modifications and human disease, Nat. Biotechnol. 28 (10) (2010) 1057–1068.
[43] A.M. Deaton, A. Bird, CpG islands and the regulation of transcription, Genes Dev. 25 (10) (2011) 1010–1022.
[44] W. Hwang, C.G. Lee, C. Lee, R. Verma, D. Rudra, Z.Y. Park, et al., Locus-specific reversible DNA methylation regulates transient IL-10 expression in Th1 cells, J. Immunol. 200 (5) (2018) 1865–1875.
[45] T. Nagasawa, CXC chemokine ligand 12 (CXCL12) and its receptor CXCR4, J Mol Med (Berl) 92 (5) (2014) 433–439.
[46] B.T. Kren, P.Y.P. Wong, A. Sarver, X. Zhang, Y. Zeng, C.J. Steer, MicroRNAs identified in highly purified liver-derived mitochondria may play a role in apoptosis, RNA Biol. 6 (1) (2009) 65–72.
[47] J. Geiger, L.T. Dalgaard, Interplay of mitochondrial metabolism and microRNAs, Cellular & Molecular Life Sciences Cmls 74 (4) (2016) 1–16.
[48] K. Ichiyama, T. Chen, X. Wang, X. Yan, B.S. Kim, S. Tanaka, et al., The methylcytosine dioxygenase Tet2 promotes DNA demethylation and activation of cytokine gene expression in T cells, Immunity 42 (4) (2015) 613–626.